Available online at www.sciencedirect.com
ScienceDirect
Thermochimica Acta 461 (2007) 4–13
thermochimica acta
www.elsevier.com/locate/tca

Review

# One hundred years research on supercooling and superheating☆,☆☆

Bernhard Wunderlich[a,b,*]

[a] *Department of Chemistry, University of Tennessee, Knoxville, TN 37996-1600, USA*
[b] *Chemical Sciences Division, Oak Ridge National Laboratory, Oak Ridge, TN 37831-6197, USA*

Available online 25 November 2006

**Abstract**

Supercooling before crystallization is well known for over 300 years and has been linked to the need of crystal nucleation. The nucleation is then followed by crystal growth, which usually quickens with increasing supercooling, goes through a maximum, and finally decreases again as the molecular mobility decreases when approaching the glass transition temperature. Superheating, in contrast, is less common. Very often melting is sufficiently fast so that its rate is determined by the conduction of the heat of fusion into the crystal, i.e., on heating, the temperature does not rise above the melting temperature until the end of the transition. Some 100 years ago, superheating was first studied. It was observed that nucleation of the mobile phase usually does not slow down the melting. Only slow melting leads to superheating. The molecular mobility increases with temperature and reduces at higher temperatures the chance of superheating. Both, supercooling and superheating are discussed on hand of theories developed for simple motifs. The results are then expanded to semicrystalline polymers which represent an arrested, metastable system with locally reversible subsystems. The macromolecules may bridge between crystal and fluid phases at points of decoupling and transfer stresses across the phase boundary. This can develop more viscous environments around the crystals. A more viscous environment, in turn, slows phase transitions, as does the need of specific conformations for the transition. Order in the amorphous phase, in contrast, increases the equilibrium phase transition, not necessarily the superheating.


*Keywords:* Superheating; Supercooling; Macromolecules; Melting; Crystallization; Kinetics; History

## Contents



## 1. Introduction

Over the past 16 years progress in calorimetry has been discussed at the Lähnwitz Seminars [1]. Since 1996, the topics changed from temperature-modulated calorimetry (TMC), to phase transitions by TMC, frequency and time dependence of heat capacity ($C_p$), thermodynamics of small systems, and the calorimetry of thin films [2].

In this paper an introduction will be given to the topic of the ninth Lähnwitz Seminar on "Transitions Far from

☆ Presented as introductory licture at the Ninth Lähnwitz Seminar on "Transitions Far from Equilibrium—Superheating; Supercooling," May 28–June 1, 2006.



* Tel.: +1 865 675 4532.
*E-mail address:* Wunderlich@CharterTN.net.

0040-6031/$ – see front matter. 
doi:10.1016/j.tca.2006.11.015

Equilibrium–Superheating; Supercooling." Supercooling, in order to crystallize, was first needed to be assessed when quantitative temperature scales were developed at the beginning of the 18th Century [3,4]. Fahrenheit, who introduced the Hg-in-glass thermometer, found it impossible to reproduce the freezing of water as a fix-point in order to follow Newton's suggestion (1701) to choose the temperatures of 0 degree at the freezing of water and 12 degree at body temperature. The cleaner the water, the more it supercooled before crystallizing. As a result, Fahrenheit chose initially a salt/ice/water mixture, which was always "dirty enough," i.e., it had enough nuclei, to immediately start crystallization and reproduce the base temperature of 0 °F for his scale. Fahrenheit also abandoned the 12°-division of Newton, it was too coarse for practical applications. He increased the resolution of his scale by a factor of eight to a body temperature of 96 °F. But Fahrenheit later recognized the problem of supercooling of pure water when it is not nucleated. He, then, redefined his scale with the freezing and boiling points of water at 32 and 212 °F, respectively, to keep earlier found data at close to the same value [5].

The story of superheating of crystals before melting began in the early 20th Century. Superheating was observed when studying melting of some feldspars that form highly viscous melts. In these cases, melting occurs so slowly that the crystals can rise by more than 150 K above their equilibrium melting temperature, $T_m^o$ [6]. Nucleation of the melt is not the answer to the description of this observation. It was recognized quickly that there are always enough nuclei on the surfaces, and particularly the edges and corners, of crystals to initiate melting close to or at $T_m^o$. If the temperature of a perfect surface or the interior of a crystal is raised above the melting point, superheating is seen, but active melting occurs at the corners and edges at $T_m^o$ [7,8]. The superheating, thus, must be linked to a slow-down or full arrest of melting. For macromolecules, superheating is more common and was discussed first for polyethylene [9].

To study superheating and supercooling, one can use the classical cooling and heating curves illustrated in Fig. 1a. They represent the simplest form of thermal analysis. The cooling curves of a liquid in the upper graph represent one experiment without transition, and one with crystallization. Without transi-

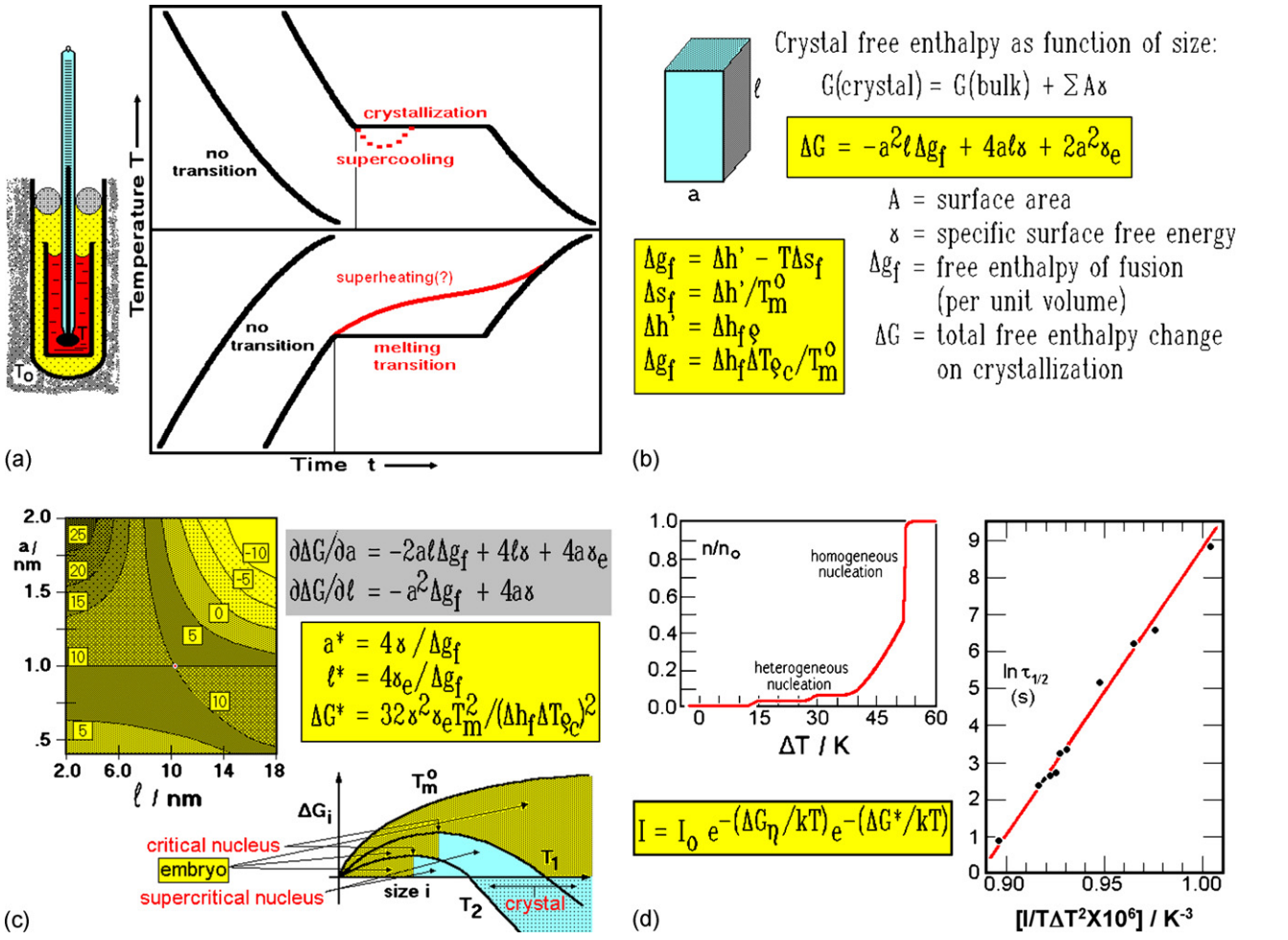


Fig. 1. (a) Simple equipment and heating and cooling curves for the crystallization and melting experiments as they were possible in the 18th Century. (b–d) Primary nucleation of crystals. (b) Equations to express the surface effect on the change in free enthalpy of crystallization, $\Delta G$. (c) Representation of $\Delta G$ as a function of the lengths $a$ and $\ell$. (d) Experiments of nucleation of polyethylene grown in dispersed droplets to minimize heterogeneous nucleation ($\tau$, half-time of primary nucleation, $\Delta T$, supercooling) [13,14].

tion, the temperature, $T$, in the well-insulated container drops exponentially with time, the slope is proportional to the heat-flow rate, $\Phi$. Newton's law of cooling: $dT/dt = K(T_o - T)$ can be linked to the change in $\Phi$, with $K$ being a constant over a wide range of temperature. On crystallization, $T$ does not become constant when $T_m^o$ is reached, instead, one notices a supercooling, which for small molecules often disappears as soon as nucleation initiates the crystal growth and the exothermic heat of crystallization reheats the sample. After appropriate calibration, the length of the drawn-out horizontal can be used to determine the heat of fusion, $\Delta H_f = -\Delta H_{crystallization}$.

The lower curves in Fig. 1a are the analogous heating curves of crystals. When $T_m^o$ is reached, superheating usually does not consist of a continuation of the heating curve as seen in the case of supercooling which, in addition, reverses in time and reaches the horizontal of equilibrium melting. Instead, the dotted curve follows an intermediate slope as drawn in analogy to the first experiments [6]. The indicated question mark is to suggest that in most cases the solid curve is followed and there is no superheating. To clarify the difference between supercooling and superheating, it is useful to first summarize the nucleation process and follow this by descriptions of crystal growth, reversible and irreversible melting.

## 2. Nucleation of crystals

Fig. 1b shows in the uppermost boxed equation the basic change of the free enthalpy of the melt on forming a crystal nucleus ($\Delta G = G_{crystal} - G_{melt}$) as a function of its size ($i = a^2\ell$). Note, that local equilibrium is assumed to be maintained all through the nucleation. The lower the mass, the higher is specific free enthalpy, $g$, due to the surface free enthalpies. The change of $\Delta G$ with dimension and time is represented in the two graphs of Fig. 1c, approximating polyethylene-like polymers (heat of fusion 210 J g$^{-1}$; end and side specific surface free energies 5.0 and 0.5 mJ cm$^{-2}$, respectively; density 1.0 Mg m$^{-3}$). The critical nucleus size is reached at the saddle point with dimensions $a^* = 1.0$ nm and $\ell^* = 10$ nm. With this critical size, the rate of nucleation can be calculated as shown in the bottom boxed equation in Fig. 1d ($I_o = 6.2 \times 10^{12}$ s$^{-1}$, a probability or entropy factor) [11]. Accordingly, the nucleation slows as $T_m^o$ of large crystals is approached, and increasingly larger critical nuclei must be reached by positive fluctuations in free enthalpy, forbidden for thermodynamic reasons. Such thermodynamic arguments about the creation of a new phase within a homogeneous fluid were already discussed by Gibbs in 1878 on the examples of liquid–liquid phase separations [12]. When approaching the glass transition temperature, $T_g$, nucleation slows because of an increased viscosity, $\eta$, in the melt. This slowing in molecular motion is described by $\Delta G_\eta$. Experiments of the nucleation of polyethylene grown in molten dispersions of droplets, sufficiently small to avoid heterogeneous nucleation in most droplets, are shown in Fig. 1d. The kinetics of the primary, homogeneous nucleation is shown in the graph on the right ($\tau$, half-time of homogeneous nucleation, $\Delta T$, supercooling) [13,14]. The heterogeneous nucleation is thought to occur on the surface of already present solid particles which are be able to support crystal growth with a lower supercooling, as seen in the graph in the upper left of Fig. 1d. Modern AFM experimentation could show, for example, that long-chain paraffins ($C_{390}H_{782}$) absorbed on graphite are able to grow ordered monomolecular layers with a 50 K higher melting temperature than their equilibrium melting temperature [15]. Such layers are able to act as effective heterogeneous nuclei. Crystallization of macromolecules was found to involve practically always heterogeneous nucleation, but still, in the presence of the most active heterogeneous nuclei, and even in the presence of crystals of already grown polymer crystals, there is no crystallization close to the equilibrium melting temperature [10].

## 3. Growth of crystals

The growth of crystals after nucleation is best characterized by microscopic measurement of the linear growth rate as a function of supercooling. Linear growth rates for several polymers are reproduced in Fig. 2a [10]. All of these show an exponential temperature dependence. The first thought was that a secondary nucleation on the surface of molecularly smooth crystals is necessary before a new layer could be initiated and, thus, would govern the crystal growth. The details of such a growth mechanism are given in Fig. 2b and c. They were developed on the model of nucleation with a reduced surface free enthalpy [16,17]. Fig. 2d, finally, illustrates the correlation between secondary nucleation for crystal growth and primary nucleation for homogeneous crystal nucleation. A match of the experiments was possible after many refinements were made [18].

An observed molecular mass segregation on crystallization of polymers with more than one length, however, represents experiments which cannot be understood with the just described nucleation and growth mechanism. To develop a thermodynamically valid approach to the segregation, it is necessary to introduce a unique barrier for the crystallization of each flexible, long-chain molecule: The molecular nucleation [19]. Fig. 3a illustrates that at a given temperature the molar mass of the longest rejected species (curves 1 and 2) does not agree with the equilibrium expected for a eutectic phase diagram (curve 3). Assuming that the fold-length governs the segregation, which may be linked to possible secondary nucleation as in Fig. 2b, is also not possible (curve 4). In order to separate different species in a multi-component system, a reversible process is necessary to sort the species by small differences in rates of entering and leaving the phases, as shown schematically in Fig. 3b. The suggestion is that if a given molecule is not sufficient to form a molecular nucleus, it is rejected by the crystal and remains in the supernatant melt or solution. Any molecule longer than needed to form a molecular nucleus would be included in the crystal as shown by completing the crystallization.

Direct evidence and the limit for molecular nucleation for flexible molecules which can melt and crystallize reversibly is shown in Fig. 3c for normal paraffins and polyethylenes of different molar mass [20]. These experiments were made using temperature-modulated differential scanning calorimetry (TMDSC) [4,21]. In the presence of crystal nuclei, the reversible melting of paraffins and mixtures of short-length

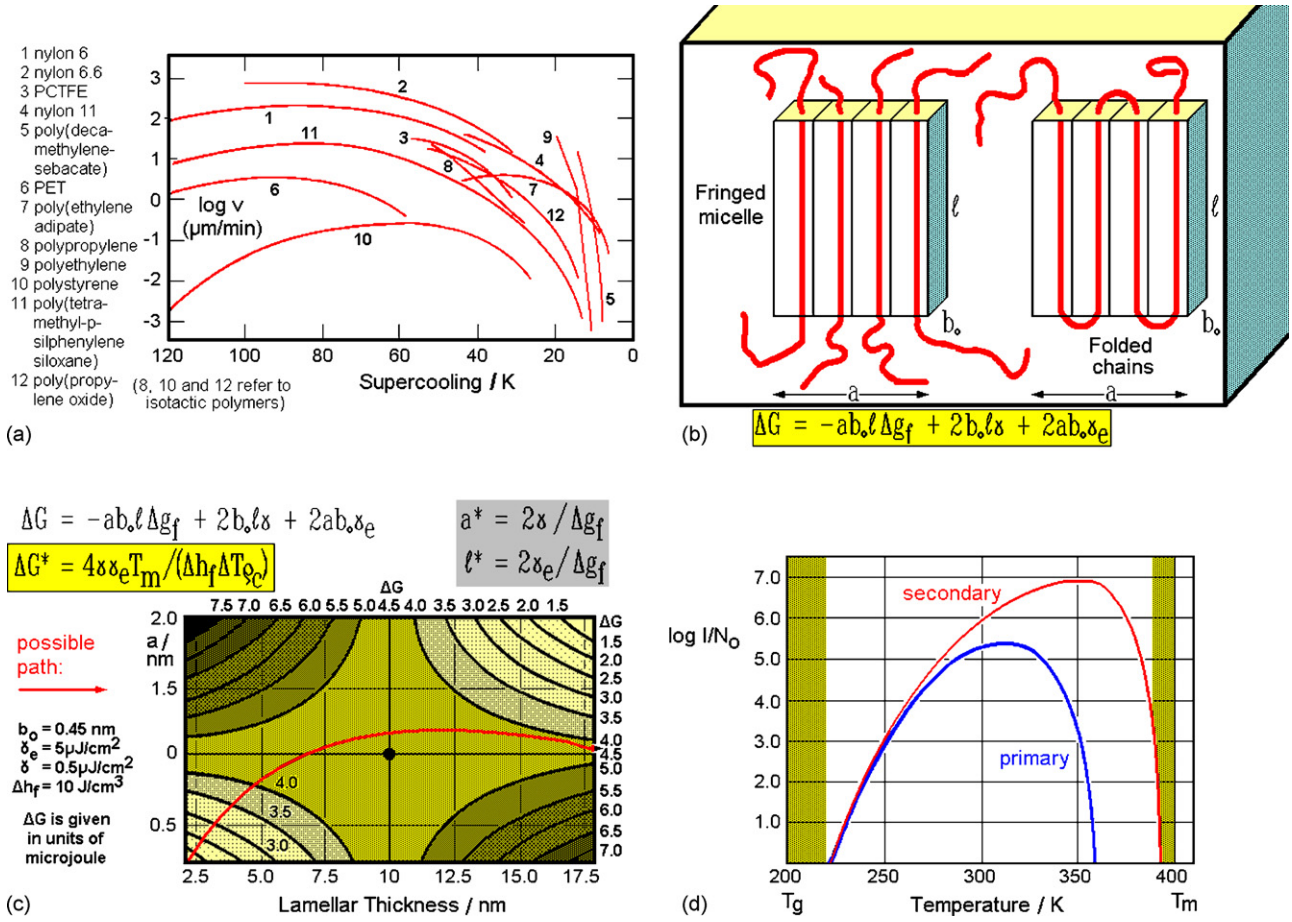


Fig. 2. Crystal growth of polymers and secondary nucleation. (a) Linear crystal growth rates, $v$, as a function of temperature for several polymers. (b and c) Schematics and equations for a secondary nucleation of polymers [16–18]. (d) Comparison of secondary and primary, homogeneous nucleation based on Figs. 2b and c and 1b–d, respectively [10].

fractions of polyethylene is seen to be limited to about 75 chain atoms, while chain-folding in crystals requires significant longer chain lengths. The marked points of decoupling in Fig. 3b separate crystalline and noncrystalline parts of the same molecule. Their detailed structure on the crystal surface is still left to speculation. Perhaps they are connected with the earlier identified inter-crystalline links or tie-molecules between grains of polyethylene [22]. In this case, the points of decoupling should reside on the upper, the fold-surface of the crystals, while the reversible melting and crystallization are expected to take place on the lateral surfaces as seen in Fig. 3b. The reversible melting of crystals of small spherical motifs in the presence of crystal nuclei is illustrated in Fig. 3d for indium [23]. The quasi-isothermal TMDSC proves the reversibility to within a few thousands of a Kelvin, limited in this experiment by the temperature lags of the calorimeter. Note that outside the (incomplete) melting and crystallization $\Phi$ is very small.

## 4. Reversible and irreversible melting

Before continuing with the discussion of superheating, it is necessary to look at a few more details of the reversible and irreversible thermodynamics of melting and crystallization [24]. For this purpose, Fig. 4a illustrates a schematic of the free energy and shows the connections between equilibrium crystal and melt, superheated crystal, and supercooled melt, and the extension of the melt to the glass. Assumed is that all nonequilibrium states are fully arrested except for the discussed changes. The annealing, perfection, and recrystallization of nonequilibrium crystals will not be described, but follows analogous paths [4]. Equilibrium, as usual, is restricted to the equilibrium crystal and the equilibrium melt, the two states of lowest free enthalpy, and the equilibrium melting at the marked intersection.

The second law of thermodynamics permits nonequilibrium changes only when they occur with decreasing free enthalpy, as exemplified by the four downward arrows for crystallization with supercooling and melting with superheating. All four arrows are described by an entropy production, $\Delta_i S$, as written in the right, boxed, bottom equation of Fig. 4a. Isothermal enthalpy changes in an isolated system, $\Delta_i H$, are forbidden by the first law of thermodynamics. This condition of $\Delta_i H = 0$ gives the direct link between $\Delta_i S$ and $\Delta_i G$. Of special interest is the nonequilibrium zero-entropy-production melting, where the metastable crystal changes to a melt of equal metastability. Formally, this is identical to equilibrium melting and can be used to assess the

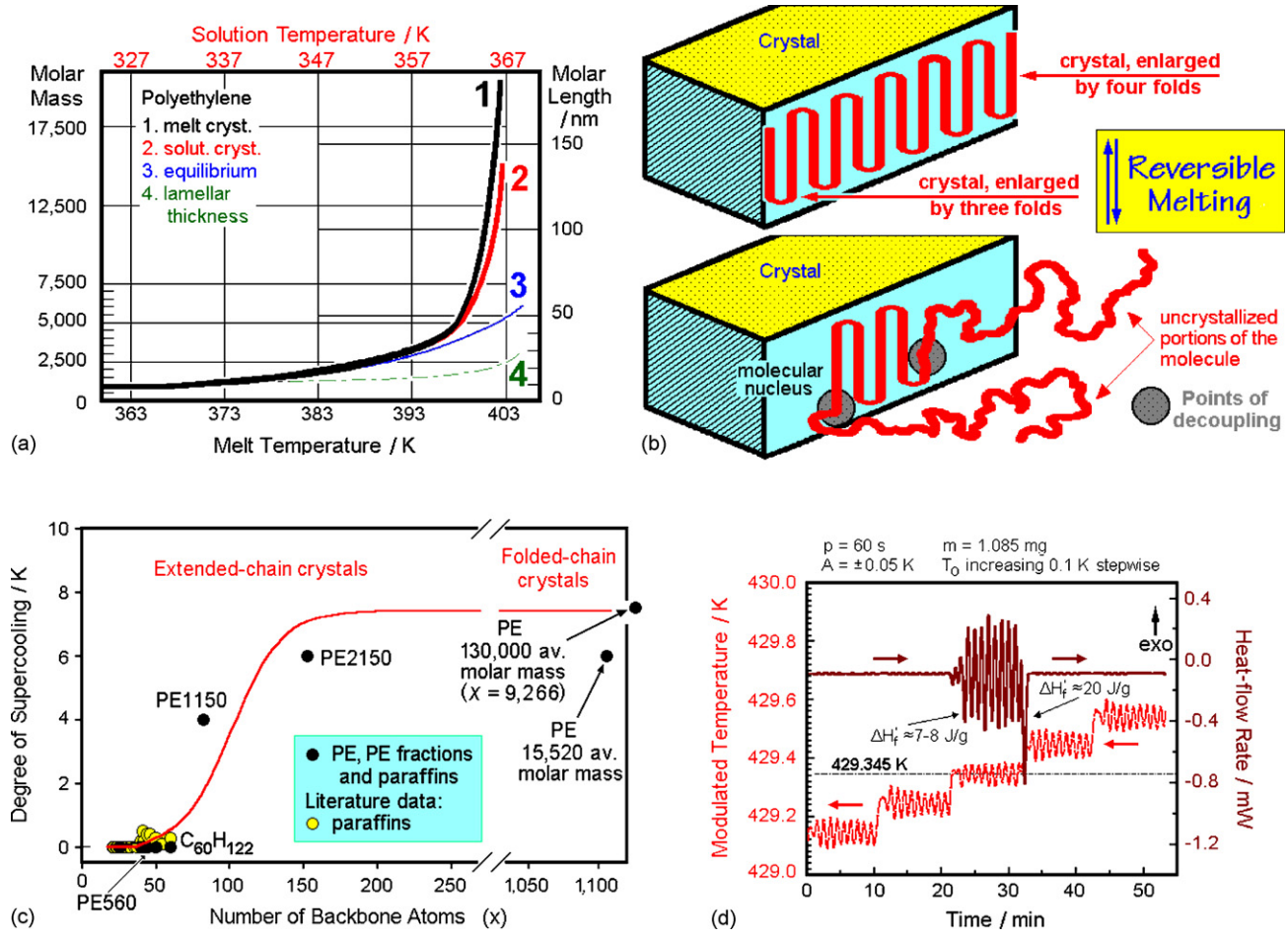


Fig. 3. Molecular nucleation and reversible melting. (a) Experiments on segregation of polyethylene on crystallization [19]. (b) Schematic of molecular nucleation and decoupling of chain segments, as it is also seen in reversible melting. (c) The change of reversible melting to irreversible melting in paraffins and polyethylene [20]. (d) Reversible melting of indium as obtained from quasi-isothermal TMDSC [23].

free enthalpy of the metastable crystal. For extrapolation, one needs to know the heat capacity of the melt as function of temperature between the equilibrium melting temperature and the zero-entropy-production melting point [24].

Fig. 4b illustrates, next, the experimental evaluation of $\Phi$ by quasi-isothermal TMDSC about the zero-entropy-production melting temperature for a low average mass poly(oxytetramethylene), POTM [25]. After each melting cycle, crystallization starts with a 2.4 K supercooling, and melting begins at the cross-over at A, i.e., this is an irreversible melting process. Crystallization does not occur at the same temperature as melting. For a full analysis, the molar mass distribution of this sample and its phase diagram have to be known, and the temperature lag of the calorimeter calibrated.

In Fig. 4c, the total melting by standard DSC of a well-crystallized poly(oxyethylene), POE, is displayed [26]. The filled circles indicate the apparent heat capacity at a large number of increasing temperatures. They indicate no reversible melting. The high molar mass PEO in Fig. 4d [27], in contrast, shows that in this case some part of the polymer melts reversibly. Such experiments reveal that the assumption of semicrystalline polymers consisting only of aggregates of nonequilibrium crystals and amorphous subsystems is incomplete. There is, in addition, a locally reversibly melting fraction at the crystal surfaces [28] which is intimately linked to molecular nucleation, as is illustrated in Fig. 3b. If the molecular nucleus has a higher melting temperature than the two decoupled chain ends, the latter can melt and crystallize reversibly.

Most theories of crystallization and melting do not consider complications in the molecular structure. They were developed for spherical motifs, such as seen in metals and salts and can be understood by assuming simple one-step transfers of the basic motifs, affected only by the surface geometry as it is described by a Kossel crystal [10]. The above-mentioned slow melting and crystallizing feldspars of high melt viscosities [6], in contrast, consist in addition to metal ions of much more complicated, covalently linked, metal–oxygen polygons which must undergo cooperative exchange of covalent bonds for mass transport. As a consequence, it was properly assumed that the larger melt viscosity contributes also to the slower mass transport across the phase boundaries, affecting $\Delta G_\eta$ in Fig. 1d. To this, the effect of probability of proper alignment on the surface for crystallization must be added, affecting the entropy factor $I_o$.

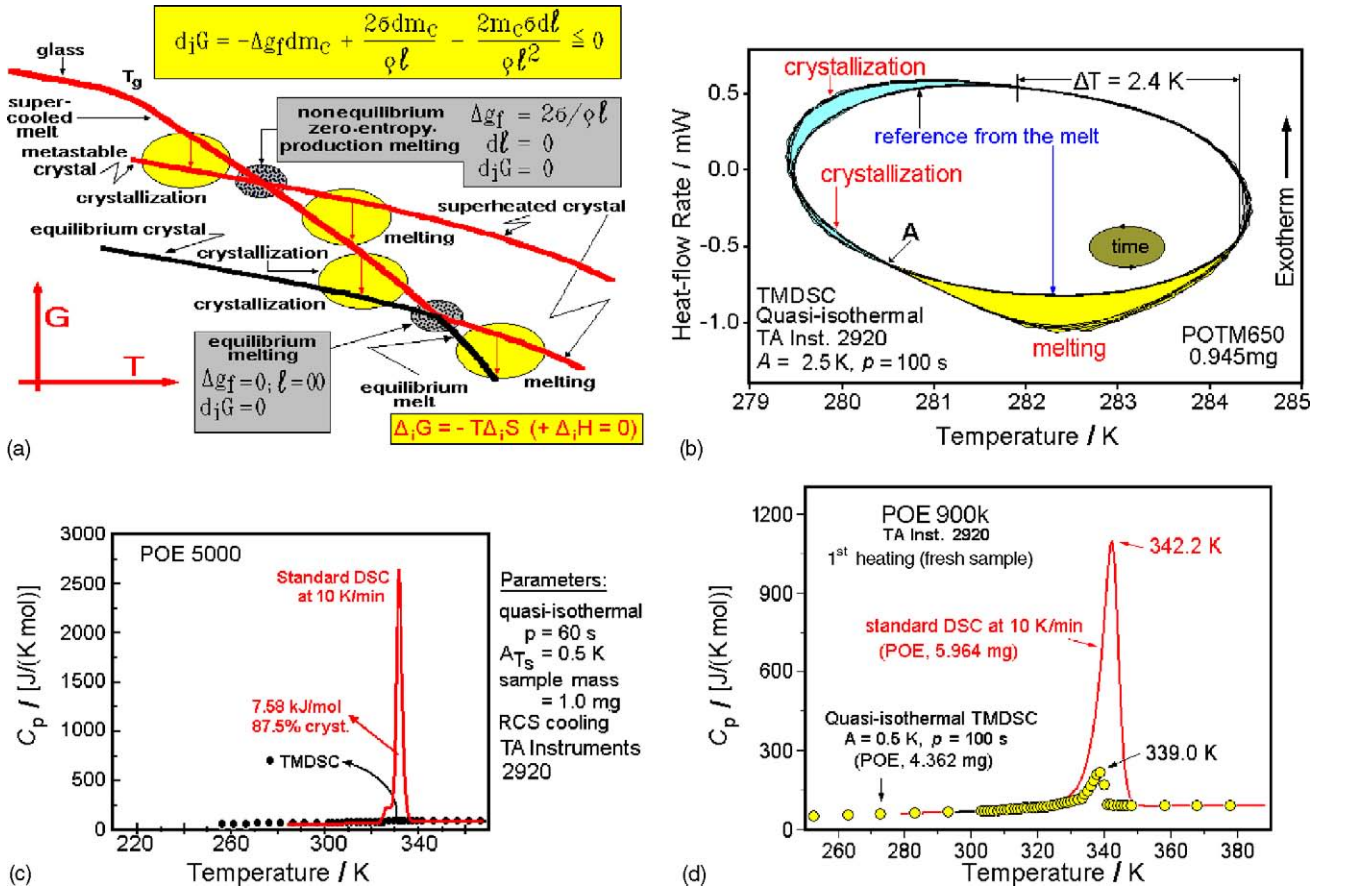


Fig. 4. Reversible, irreversible, and locally reversible melting. (a) Free enthalpy diagram of equilibrium and nonequilibrium states [24]. (b) Crystallization with supercooling and melting of an oligomer fraction of POTM, measured by quasi-isothermal TMDSC (Lissajous figure of $\Phi$ vs. temperature) [25]. (c and d) Irreversible and locally reversible melting for semicrystalline poly(oxyethylene), POE, of low and high molar mass [26,27].

## 5. Superheating

With the information from the prior section one can turn to a discussion of superheating. First, it is necessary to try to understand the melting mechanism. Again, macromolecules are perhaps the most studied class of molecules which may superheat because of their long-chain structure and macroconformation [4]. As stated already by Tammann in 1910 [10]: "Crystals above the melting temperature can only be realized when they are in the process of melting . . . [since] the number of points which can initiate melting of a crystal is extraordinarily large in comparison to those points where crystallization of a liquid is initiated." For macromolecules this idea of nucleation of melting caused by the surface defects was supported by large-scale molecular dynamics simulation of polyethylene crystals approaching the melting temperature [29,30]. The chain ends residing in the surface were seen to carry out large excursions by leaving the crystal surface, quite similar to the schematic in Fig. 3b.

The first observation on superheating of polyethylene [9] was immediately followed by structural and kinetic studies of such melting using electron microscopy [31,32]. Fig. 5 illustrates replicas of fracture surfaces of crystals in different stages of melting. In Fig. 5a the reference extended-chain crystal lamellae are seen. They were grown at elevated pressure and replicated after pressure release. The polyethylene was 98% crystalline as measured by calorimetry. As melting progressed, different samples were quenched, so that poor folded-chains crystals grew from the molten portions. These folded-chain lamellae have a thickness of less than 20 nm and show on replication no comparable structure to the not yet melted, extended-chain crystals. The smallest lamellae melt first and at lower temperature (Fig. 5b). The larger lamellae start to melt from their growth faces and with only a limited amount of break-up of the original lamellae (Fig. 5c). Finally, after a very long time at the equilibrium melting temperature when a crystallinity of only 0.1% remained, one can still see a rare, left-over lamella (Fig. 5d). This lamella is still of the same thickness and structure as before, and micrometers in width, proving that no thinning of the lamellae occurs and melting proceeds on the growth faces.

The kinetics of superheating of extended-chain crystals of high-molar-mass, strictly linear polymethylene is illustrated in Fig. 6a for different temperatures above the $T_m^o$ of 414.6 K. The reason for the superheating is the slow melting caused by the need of melting to start either at a chain end or at a fold at the surface of the crystal. Both of these are rare in extended-chain crystals of high-molar-mass. To establish the sharp equilibrium melting point of this polymer, dilatometry was used with successive measurements spaced by 24 h.

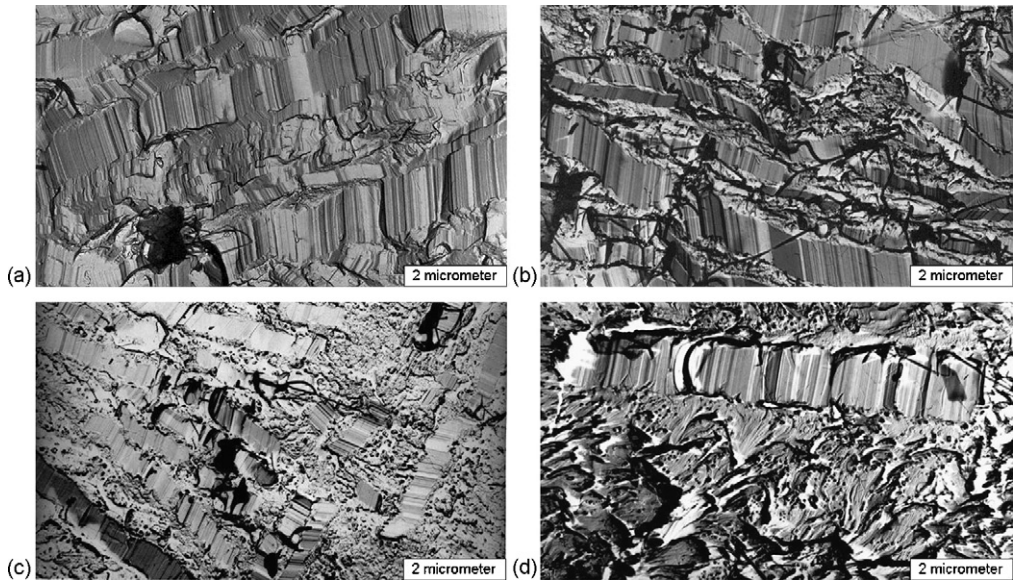


Fig. 5. Polymer melting mechanism of extended-chain lamellae of polyethylene of an average molar mass of 153,000 Da and a polydispersity of 18. (a) Fracture-surface of 98% crystallized polyethylene, $T_m^o = 411.4$ K. (b) Sample in (a) after heating to 410.6 K, remaining crystallinity 47%. (c) Sample in (a) after heating to 411.4 K, for 2.3 h, remaining crystallinity 26%. (d) Sample in (a) after heating to 411.4 K for 100 h, remaining crystallinity 0.1%.

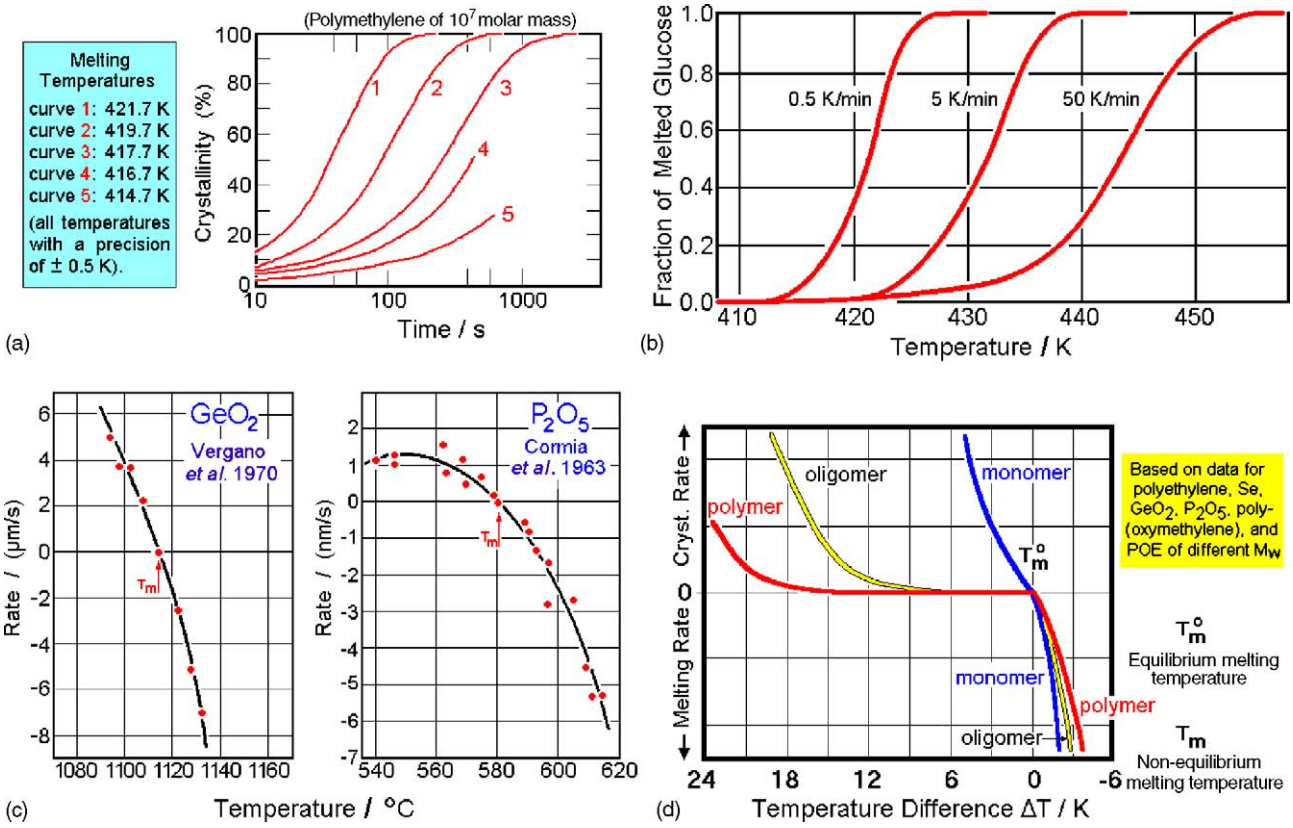


Fig. 6. Superheating of crystals. (a) Change of crystallinity with time of extended-chain crystals of a strictly linear polymethylene of high molar mass at various temperatures above the equilibrium melting temperature ($T_m^o = 414.6$ K) [9]. (b) Fraction of melted glucose on thermal analysis at different heating rates [9]. (c) Melting kinetics of germanium dioxide and phosphorous pentoxide as represented by the linear rate of melting of the crystals [34,35]. (d) Summary of melting and crystallization rates of various crystals.

Folded-chain crystals of polyethylene are typically of 10–30 nm thickness and of lower molar mass, in contrast, they show no superheating under comparable conditions of measurement [9,33]. Every chain end or fold can initiate melting if it lies on a crystal surface. Delays, however, can arise if the chain ends are buried inside the crystal, or, even more effectively, inside neighboring, higher melting crystals.

Fig. 6b reproduces the melting of the small molecule glucose, first shown to superheat by Tammann with heating curves [10], and repeated later by using differential thermal analysis [9]. The curves indicate that melting starts when the equilibrium melting point is reached, but the crystals are easily superheated because of slow melting. In this case, one expects that the H-bond structure, which also is at the root of the high viscosity of the molten glucose, is the cause of the slow melting.

Fig. 6c illustrates the microscopic measurement of the linear crystallization and melting rates of germanium dioxide and phosphorous pentoxide [34,35]. Of interest for these two oxides are the finite slopes through the equilibrium melting temperature. In Fig. 6d these data are compared to polymers. The macromolecules have wide, horizontal discontinuity of the crystallization rate due to molecular nucleation. The polymers have typically a 10–50 K temperature range below the equilibrium melting in which the melt is metastable and cannot be nucleated by adding of crystals. The finite melting or crystallization rates outside this range of metastability permit then superheating or increased supercooling if the heat conduction into or out of the sample is faster than the phase transition.

Several other observations affecting the melting of polymers are illustrated in Fig. 7 and document the importance of the decoupling concept of long-chain molecules. Fig. 7a shows the apparent heat capacity by standard DSC of $a \approx 30\%$ crystalline poly(oxy-2,6-dimethyl-1,4-phenylene), PPO [36]. At the beginning of melting, practically the complete amorphous fraction is still rigid (in form of a rigid-amorphous fraction, RAF). More detailed analysis is possible with quasi-isothermal TMDSC. It shows the glass transition of the RAF occurs at a 20 K higher temperature (●) than for the fully amorpous sample (482 K). Earlier annealing studies revealed that the semicrystalline sample reduced its crystallinity at 493.2 K to 9.3% in 20 h, at 505.2 K to 1.5% in 1 h [37]. The conclusion is that the PPO actually superheats. The melting rate is determined by the slow rate of molecular motion of the glassy RAF at the interface. Only after the RAF has become mobile at the point of decoupling, also shown in Fig. 7a, can the melting begin. On expects the $T_m^o$ of PPO to be $495 \pm 5$ K. This is an example of superheating by enclosing the crystal in a molecularly attached glass. Just as small molecules do not start melting from inside a perfect crystal, glass-enclosed polymer crystals cannot melt below $T_g$ of the glass. The PPO superheats by ≈20 K for the time-scale of the standard DSC experiment.

Another type of superheating is illustrated in Fig. 7b [38]. The DSC traces illustrate the change of the melting of undrawn and drawn polyethylene. On drawing, the crystals of the originally undrawn fiber are deformed from a lamellar to a fibrillar morphology with many inter-crystalline links. The crystals are expected to become less perfect on such major deformation, but still the melting temperature increases, seemingly leading to superheating. It needs to be explained why on drawing, the melting peak increases in temperature, and why the fiber held at constant length has an even higher, but broader melting peak than the one which is free to shrink. The answer becomes clear when one inspects Fig. 7c. Here the melting of radiation cross-linked *cis*-1,4-poly(2-methylbutadiene), natural rubber, is analyzed by force–length–temperature measurements [39]. These measurements are analogous to the determination of pressure–volume–temperature diagrams. The link to calorimetry is given by the two respective Clausius–Clapeyron equations written in the figure. The melting temperature of a crystal in contact with an oriented melt has a lower entropy of fusion and, thus, a higher melting temperature, just as the melting temperature usually increases with increasing hydrostatic pressure. Under such conditions, $T_m^o$ increases. As long as this is the only effect, there is no superheating.

Returning to Fig. 7b one must note that there is no external force kept on the drawn sample. But, the crystals within the drawn fiber keep the amorphous fractions partially oriented, i.e., the overall structure is held by the oriented crystals, coupled molecularly to the melt which can disorient only after some of the crystals melt. After this initial melting, the crystals are now superheated and can melt fast. In some cases, the heat of fusion is absorbed so quickly, that the fiber actually cools and has then a retrograde melting peak. This collapse of the crystals on reaching a superheated state explains the sharper melting peak despite the crystals not being any more perfect than the undrawn fibers. This dismantling of the crystal scaffold on melting is more strongly hindered in the experiment at constant length, so that in this case the melting peak remains broad and is shifted to even higher temperature [33]. Overall, the melting of drawn polymer fibers cannot maintain the local equilibria, and the overall melting is irreversible. For more detailed information, quantitative TMDSC is needed to identify the various phases and their changing state of deformation.

The last graph in Fig. 7d illustrates the analysis of the $C_p$ of ultrahigh-molar-mass, gel-spun polyethylene, UHMMPE, in the pre-melting region [40]. The fiber is of very high strength and high orientation in the non-crystalline fraction. The UHMMPE is extended 10× as much as the drawn fibers of Fig. 7b. Because of the many irreversible processes in the major melting region, the discussion is limited to temperatures below 400 K. Up to this limit in temperature, little reorganization takes place and by subtracting the experimental $C_p$ of the 100% crystalline polyethylene one can judge the glass transition of the mobile portion of the fiber from the $\Delta C_p$ given in the lower curves. Of the two types of fibers, A is as drawn, and B is annealed after drawing. The bottom graph shows the glass transitions of these two fibers. As is expected, there is a larger increase in heat capacity for the fiber A and a smaller one for fiber B which has the higher crystallinity. Adding the crystallinity from the heat of fusion and the percentage of amorphous fraction from $\Delta C_p$, as listed in the figure, the total is larger than 100%. The conclusion reached is that the amorphous fraction has a sufficiently high orientation so that it can contribute to the heat of fusion due to an entropy of disordering on melting the fiber and can

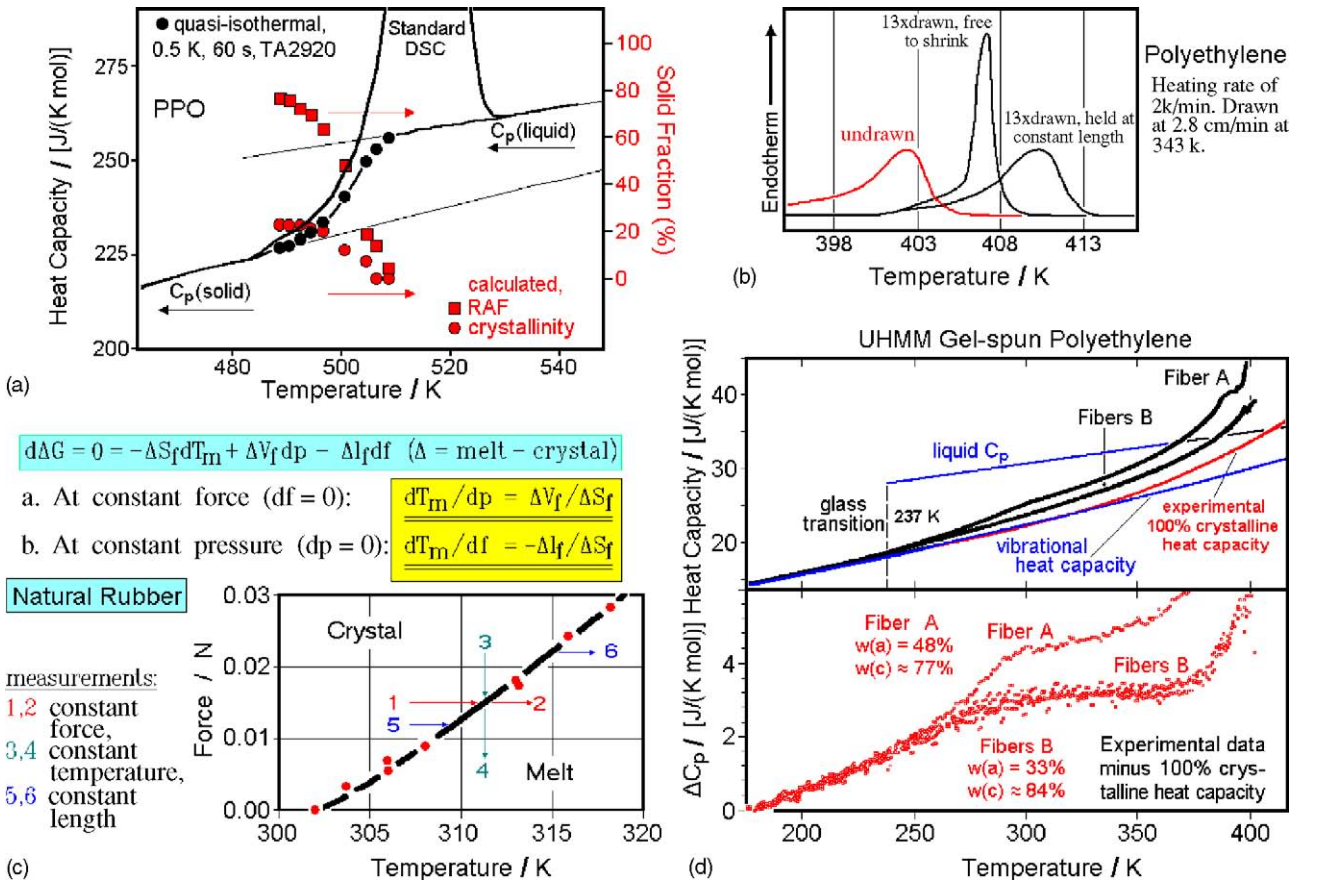


Fig. 7. Coupling and decoupling between crystals and noncrystalline phases. (a) Melting and glass transition of semicrystalline PPO deduced from the apparent $C_p$ measured by DSC at 10 K min$^{-1}$ (left scale) and the fractions of RAF and crystallinity measured by TMDSC (right scale). (b) Standard DSC of undrawn and drawn polyethylene [38]. (c) Change of the melting temperature of natural rubber measured at constant external force (1 → 2), constant temperature (3 → 4), and length (5 → 6) [39]. (d) Heat capacity of ultra-high molar-mass, gel-spun polyethylene [40].

contribute to the higher melting temperature observed for these fibers. Other measurements by X-ray diffraction and solid state NMR could verify that, indeed, there is a melt with an orientation approaching that of the crystal and this fraction has a mobility which is intermediate between crystal and the melt. With these fractions identified, time-dependent melting experiments may unravel more of these complicated locally reversible changes of melting temperature and irreversible processes of superheating, which in the case of UHMMPE may also include changes to different crystal structures.

It is obvious from the examples discussed, that it would be of value to spend more effort on the study of superheating and supercooling of the various types of molecules and transitions from the point of view or equilibrium and irreversible thermal properties.

## 6. Conclusions

Superheating and supercooling are basic phenomena which need to be described using irreversible thermodynamics and can be studied by the various forms of thermal analysis. Of particular use for the study of reversibility is temperature-modulated calorimetry. Supercooling is a frequently seen phenomenon identified already some 300 years ago. It is caused mainly by primary nucleation. In a nucleated melt or solution, supercooling may still exist when a special mechanism of the subsequent crystal growth lowers the temperature of measurable growth. Such a growth mechanism for polymers, for example, is caused by the need of molecular nucleation. Superheating is rarely caused by the need of nucleation of the disordered phase since the crystal edges and corners are sufficiently disordered to serve as their nuclei for the melt. This leaves for the superheating only the second cause, an inherent transition mechanism which allows fast melting only at higher temperature. If the amorphous phase involved in the transition is highly viscous so that the molecular motion is slow, or if the molecular rearrangement to the new phase is slowed or arrested, superheating may be observed. Examples of several different processes were collected from the literature of the last 100 years and are given in this paper as they were presented at the ninth Lähnwitz Seminar.

## Acknowledgements

This work was supported by the Division of Materials Research, National Science Foundation, Polymers Program, Grant# DMR-0312233. Use of some of equipment and laboratory space was provided by the Division of Materials Sciences and Engineering, Office of Basic Energy Sciences, U.S. Depart-

ment of Energy at Oak Ridge National Laboratory, managed and operated by UT-Battelle, LLC, for the U.S. Department of Energy, under contract number DOE-AC05-00OR22725.

## References

[1] C. Schick, Universität Rostock, Fachbereich Physik, Arbeitsgruppe Polymerphysik, and G.W.H. Höhne, Gesellschaft für Thermische Analyse e.V. (GEFTA), Arbeitskreis Kalorimetrie. Biannual meetings since 1990.
[2] Published, in sequence, Thermochim. Acta 304/305 (1997); 330 (1999); 377 (2001); 403 (2003); 432 (2005).
[3] For historical notes, basic descriptions of the underlying theories, and references to the early literature see reference [4] or the computer course: "Thermal Analysis of Materials." Available by downloading through the Internet site: http://web.utk.edu/athas, or via the European Virtual Institute for Thermal Metrology: http://www.evitherm.org/index.asp at their home page for thermal analysis and calorimetry or on CD from the author.
[4] B. Wunderlich, Thermal Analysis of Polymeric Materials, vol. 894, Springer-Verlag, Berlin, 2005, xvi p. (947 figures).
[5] In some countries temperature is still measured in degrees fahrenheit. These are considered to be the more practical for day-to-day use than the temperature in Kelvin. Changes by less than one degree are barely noticeable in °F, making it unnecessary to know about decimals. Furthermore, temperatures below zero happen rarely and are dangerously cold, so that negative numbers have not really to be dealt with, while a body-temperature above 100 °F signals an illness that needs attention.
[6] L. Day, E.T. Allen, J.P. Iddings, The Isomorphism and Thermal Properties of the Feldspars, Carnegie Institution of Washington, Washington, 1905.
[7] G. Tammann, Z. Phys. Chem. 68 (1910) 257.
[8] M. Volmer, O. Schmidt, Z. Phys. Chem. B35 (1937) 467.
[9] E. Hellmuth, B. Wunderlich, J. Appl. Phys. 36 (1965) 3039.
[10] For a detailed description of "Crystal Nucleation, Growth, Annealing," see: B. Wunderlich, Macromolecular Physics, vol. II, Academic Press, New York, 1976, available as PDF reprint with the computer course of [3].
[11] D. Turnbull, J.C. Fisher, J. Chem. Phys. 17 (1949) 71.
[12] J.W. Gibbs, Trans. Conn. Acad. 3 (1878) 343.
[13] R.L. Cormier, F.P. Price, D. Turnbull, J. Chem. Phys. 37 (1962) 1333.
[14] F. Gornick, G.S. Ross, L.J. Frolen, J. Polym. Sci. Part C 18 (1967) 79.
[15] S.N. Magonov, N.A. Yerina, G. Ungar, D.H. Reneker, D.A. Ivanov, Macromolecules 36 (2003) 5637.
[16] J.D. Hoffman, J.J. Weeks, W.M. Murphy, J. Res. Nat. Bur. Stand. 63A (1959) 67.
[17] F.P. Price, J. Chem. Phys. 31 (1959) 1679.
[18] J.P. Armistead, J.D. Hoffman, Macromolecules 35 (2002) 3895.
[19] B. Wunderlich, A. Mehta, J. Polym. Sci. Polym. Phys. Ed. 12 (1974) 255.
[20] J. Pak, B. Wunderlich, Macromolecules 34 (2001) 4492.
[21] M. Reading, D.J. Hourston (Eds.), Modulated-temperature Differential Scanning Calorimetry, Springer, Dordrecht, The Netherlands, 2006.
[22] H.D. Keith, F.J. Padden Jr., R.J. Vadimsky, Science 150 (1965) 1026.
[23] K. Ishikiriyama, A. Boller, B. Wunderlich, J. Therm. Anal. 50 (1997) 547.
[24] B. Wunderlich, Polymer 5 (125) (1964) 611.
[25] J. Pak, M. Pyda, B. Wunderlich, Thermochim. Acta 296 (2003) 43.
[26] K. Ishikiriyama, B. Wunderlich, Macromolecules 30 (1997) 4126.
[27] W. Qiu, M. Pyda, E. Nowak-Pyda, A. Habenschuss, B. Wunderlich, Macromolecules 38 (2005) 8454.
[28] B. Wunderlich, Progr. Polym. Sci. 28 (2003) 383.
[29] B.G. Sumpter, D.W. Noid, G.L. Liang, B. Wunderlich, Adv. Polym. Sci. 116 (1994) 27, Fig. 7. For details on the specific crystal simulations see [30].
[30] G.L. Liang, D.W. Noid, B.G. Sumpter, B. Wunderlich, Acta Polym. 44 (1993) 214.
[31] R.B. Prime, B. Wunderlich, L. Melillo, J. Polym. Sci. Part A-2 7 (1969) 2091.
[32] R.B. Prime, B. Wunderlich, J. Polym. Sci. Part A-2 7 (1969) 2063–2073.
[33] For a detailed description of "Crystal Melting," see: B. Wunderlich, Macromolecular Physics, vol. III, Academic Press, New York, 1980, available as PDF reprint with the computer course of [3].
[34] P.J. Vergano, D.R. Uhlmann, Phys. Chem. Glasses 11 (1970), 30 and 39.
[35] R.L. Cormia, J.D. Mackenzie, D. Turnbull, J. Appl. Phys. 34 (1970) 2239.
[36] J. Pak, M. Pyda, B. Wunderlich, Macromolecules 36 (2003) 495.
[37] S.Z.D. Cheng, B. Wunderlich, Macromolecules 20 (1987) 1630.
[38] K.-H. Illers, Angew. Makromol. Chem. 12 (1970) 89.
[39] J.F.M. Oth, P.J. Flory, J. Am. Chem. Soc. 80 (1958) 1297.
[40] Y.K. Kwon, A. Boller, M. Pyda, B. Wunderlich, Polymer 41 (2000) 6237.